Journal of Information Display, vol. 3, no. 3, 2002

Multi-view Display with Hologram Screen using Three-dimensional Bragg Diffraction

Masaaki Okamoto[a] **and Eiji Shimizu**[b]

Abstract

Multi-view function is important to three-dimensional displays without dedicated glasses. It is the reason that the observers earnestly desire to change their positions freely. Multi-viewing is also principal to the reality of three-dimensional (3D) image displayed on the screen. The display of projection type has the advantage that the number of viewing points can be easily increased according to the number of projectors. The authors research on multi-view projection display with hologram screen. Powerful directionality of the diffracted beam from hologram screen is required unlike two-dimensional (2D) display. We developed a new method that all diffracted beams satisfied the same Bragg condition and became sufficiently bright to observe the 3D image under usual indoor light. The principle is based on the essential Bragg diffraction in the three-dimensional space. Owing to such three-dimensional Bragg diffraction we achieved an excellent hologram screen that could be multiple reconstructed in spite of single recording. This hologram screen is able to answer arbitrary numbers of viewing points within wide viewing zone. The distortion of 3D image becomes also sufficiently small with the method of dividing the cross angle between illumination and diffraction beam.

Keywords : multi-view display, 3D display, hologram screen, bragg diffraction.

1. Introduction

Binocular stereoscopic displays with special glasses are preceding the other types in the field of 3D displays because several systems of virtual reality become noticed. Binocular display is not recommended to use for long time from the standpoint of human vision. Multi-view display without dedicated glasses is more desirable. Multi-view function is also remarkably effective to increase the reality of 3D image. Though full-parallax display like hologram is ideal, electro-holography is not yet practical [1-3]. The types that widely distribute small pixels of those screens are developed by many researchers [4-8]. Nevertheless there is fundamental weakness of the resolution about the distribution type. The projection type is free from such difficulty and moreover has the advantage that the number of viewing points can be easily increased according to the number of projectors.

Newswanger initially proposed a multi-view display of projection type using hologram screen [9]. His proposal was a hologram screen that was multiple recorded and multiple reconstructed in accordance with the number of viewing points. In this case it is well known that the brightness of the diffracted beam is degraded to $1/N$ or $1/N^2$ (N means the number of exposures) [10]. Our trial hologram screen exposed only 4 times also resulted in failure [11]. Powerful directionality and remarkable brightness of the diffracted beam is required in 3D display unlike 2D display. It is unfortunate that multi-recorded hologram is not adequate

Manuscript received June 27, 2002; accepted for publication September 22, 2002.

a. Laboratories of Image Information Science and Techno logy WTC-18F, Mailbox-114, 1-14-16 Nanko-kita Suminoe-ku, Osaka 559-0034, Japan.
b. Department of Electrical Engineering, Osaka City University 3 -3-138, Sugimoto Sumiyoshi-ku, Osaka 558-0022, Japan.
E-mail : okamoto@list.mado.or.jp **Tel** : +81 6-6616-5008
Fax : +81 6-6616-5009

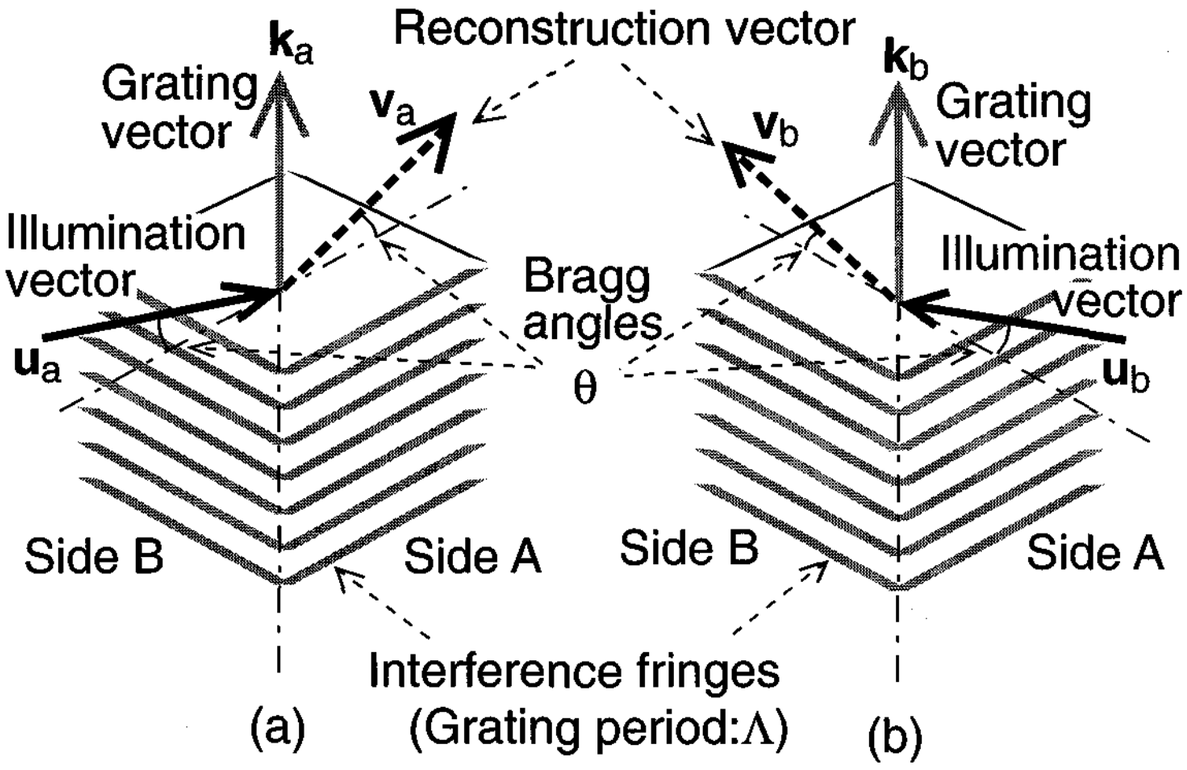

Fig. 1. Principle of three-dimensional Bragg diffraction.

for multi-view projection screen. Though holography is utilized for controlling the direction of beam emitted from light source, many researchers direct their schemes toward the distribution types [5-8].

We continued to research on hologram screen of projection type and paid attention to the angular selectivity of hologram [12]. We pointed out that even single recorded hologram could be multiple reconstructed by the illuminations near the Bragg angle. This projection screen was effective among the narrow angular selectivity of volume hologram. Thus we reached the entrance of multi-view hologram screen of projection type [13].

Next we investigated the nature of the Bragg diffraction in the three-dimensional space. We found the interesting principle that the Bragg angle is kept at the same value even if the direction of illumination is rotated around the grating vector [14]. The basis of this idea is the fact that the interference fringes are composed of two-dimensional planar layers in the three-dimensional space. Owing to such three-dimensional Bragg diffraction we achieved an excellent hologram screen that could be multiple reconstructed in spite of single recording [15]. All diffracted beams satisfied the same Bragg condition and became sufficiently bright to observe 3D image under usual indoor light. This hologram screen is able to answer arbitrary numbers of viewing points within wide viewing zone.

In this paper we introduce the method to extend the theory of the Bragg diffraction to the three-dimensional space. We explain the algorithm to convert the directions of a pair of illumination and diffracted beam under the condition that the grating vector becomes the axis of rotation. Then we introduce a design of multi-view display with hologram screen and show our experimental result of 4 viewing points.

2. Three-Dimensional Bragg Diffraction

Volume hologram is suitable to control the direction of the beam diffracted by the hologram screen. It is important to provide the specific picture projected on the screen for the corresponding viewing area. The diffraction efficiency of volume hologram reaches the highest value when half of the cross angle between illumination and diffracted beam becomes equal to the Bragg angle of the grating [10, 16-18]. This best diffractive condition is called the Bragg condition.

Normally the Bragg condition is discussed like two-dimensional phenomenon in the cross section of three-dimensional volume hologram. This procedure is proper in the case where the common plane containing both illumination and diffracted beam is perpendicular to the hologram screen. When the common plane is not perpendicular to the hologram screen, the total optical path through the illumination and the diffracted beam must be considered in the three-dimensional structure. In this case the Bragg condition can not be discussed in a single two-dimensional plane and must be analysed with

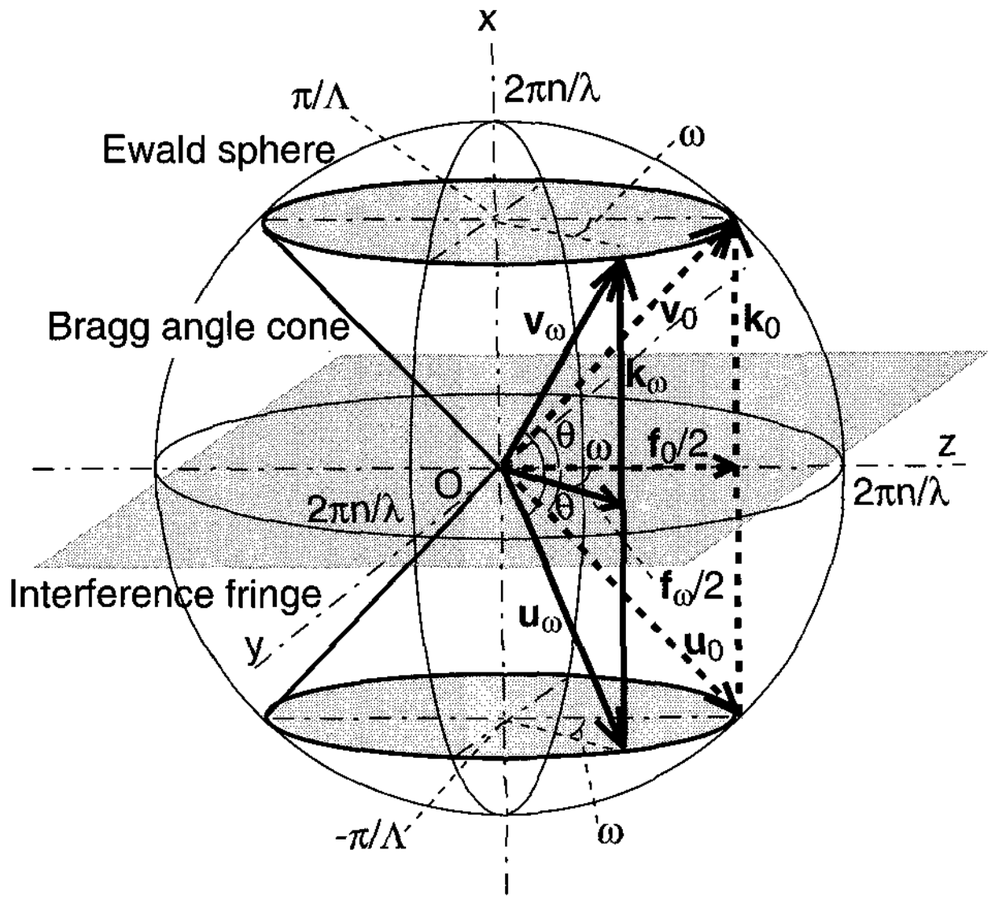

Fig. 2. Ewald sphere and Bragg angle cone.

the geometry of three-dimensional space.

We first examine a simple model of three-dimensional Bragg diffraction. Fig. 1 illustrates two cases of the Bragg diffraction about the same volume hologram. The layers piled with squares show interference fringes. The case (a) shows the state where the optical path is parallel to the side A of the interference fringes; (b) shows the case parallel to the side B. The grating vector is showed by $\mathbf{k}_a$ or $\mathbf{k}_b$ which size is $2\ \pi/\Lambda$. Λ is the grating period of fringes. The vector $\mathbf{u}_a$ or $\mathbf{u}_b$ shows the illumination vector which size is $2\ \pi n/\lambda$. λ is the wavelength of the illumination and n is the refractive index of this hologram. The vector $\mathbf{v}_a$ or $\mathbf{v}_b$ shows the reconstruction vector of diffracted beam which size is also $2\ \pi n/\lambda$. It is supposed that both the illumination and the diffracted beam satisfy the Bragg condition. The Bragg angle is expressed by θ. The Bragg condition becomes

$$|\mathbf{v}-\mathbf{u}| = \frac{4\pi n}{\lambda}\sin(\theta) = |\mathbf{k}| = \frac{2\pi}{\Lambda} \qquad (1)$$

where all suffixes are eliminated [19, 20]. Equ. (1) is satisfied in each case, (a) or (b). Two grating vectors $\mathbf{k}_a$ and $\mathbf{k}_b$ are equivalent in size and direction. Equ. (1) does not depend on the direction from which the fringes are recorded by a pair of object beam and reference beam. Moreover equ. (1) is satisfied in the case where the pair of illumination vector **u** and reconstruction vector **v** is rotated by arbitrary angle around the grating vector **k**.

We can conclude that there are countless pairs of illumination and diffracted beam that satisfy the same Bragg condition. Such pairs exist on the cone which complementary angle is the Bragg angle and which central axis is on the grating vector **k**. We call this cone the Bragg angle cone. An arbitrary pair of illumination and diffracted beam shapes a longitude of the Bragg angle cone that is the line crossed by the cone and the plane containing the central axis. The existence of countless pairs is the theoretical basis of our multi-view hologram screen that is single recorded and multiple reconstructed.

3. Algorithm of Rotation

In this chapter we explain the algorithm to rotate the directions of a pair of illumination and diffracted beam on the Bragg angle cone by an arbitrary angle around the grating vector. Fig. 2 shows Ewald sphere used in crystal optics [21, 22]. The coordinates of Ewald sphere are illustrated in the reciprocal space. The radius of Ewald sphere is indicated by the inverse of the wavelength λ; the value is $2\ \pi n/\lambda$. For convenience it is assumed that the surface of interference fringe is parallel to the yz-plane. The grating vector $\mathbf{k}_0$ corresponds to this grating. In the reciprocal space the distance between the

neighboring fringes is shown by π/Λ where Λ is the grating period. Then the length of grating vector $\mathbf{k}_0$ becomes $2\pi/\Lambda$. $\mathbf{u}_0$ shows the illumination vector before rotation and $\mathbf{v}_0$ shows the reconstruction vector before rotation. We define a new vector $\mathbf{f}_0$ which is the sum vector of $\mathbf{u}_0$ and $\mathbf{v}_0$. We call $\mathbf{f}_0$ the fringe vector. The cross angle between $\mathbf{u}_0$ and $\mathbf{f}_0$ is the Bragg angle θ. The cross angle between $\mathbf{f}_0$ and $\mathbf{v}_0$ is also the same Bragg angle θ.

Next we examine the rotation angle ω. After rotation ω, $\mathbf{u}_0$ reaches $\mathbf{u}_\omega$, $\mathbf{v}_0$ reaches $\mathbf{v}_\omega$, $\mathbf{f}_0$ reaches $\mathbf{f}_\omega$ and $\mathbf{k}_0$ reaches $\mathbf{k}_\omega$. $\mathbf{u}_0$ and $\mathbf{u}_\omega$ exist on the same Bragg angle cone. $\mathbf{v}_0$ and $\mathbf{v}_\omega$ exist on the other conjugate Bragg angle cone. The target of our analysis is to get the value of $\mathbf{u}_\omega$ and $\mathbf{v}_\omega$ from the value of $\mathbf{u}_0$, $\mathbf{v}_0$ and ω. Here we adopt the notation (u_{0x}, u_{0y}, u_{0z}) about the components of the illumination vector $\mathbf{u}_0$. Each component expresses the x-coordinate, the y-coordinate or the z-coordinate of $\mathbf{u}_0$. We also adopt notations like $\mathbf{u}_0$ to the other vectors as the need arises.

The grating vector $\mathbf{k}_0$ and the fringe vector $\mathbf{f}_0$ are expressed as following equations by the illumination vector $\mathbf{u}_0$ and the reconstruction vector $\mathbf{v}_0$.

$$\mathbf{k}_0 = \mathbf{v}_0 - \mathbf{u}_0, \mathbf{f}_0 = \mathbf{v}_0 + \mathbf{u}_0 \qquad (2)$$

The Bragg condition and/or the Bragg angle θ of equ. (1) are/is implicitly included in equ. (2). The relation between the fringe vector before rotation and that after rotation is expressed as follows.

$$\cos(\varpi) = \frac{\mathbf{f}_0 \mathbf{f}_\varpi}{|\mathbf{f}_0||\mathbf{f}_\varpi|} = \frac{f_{0x} f_{\omega x} + f_{0y} f_{\omega y} + f_{0z} f_{\omega z}}{|\mathbf{f}_0|^2} \qquad (3)$$

It is because the absolute value of $\mathbf{f}_\omega$ is equal to the absolute value of $\mathbf{f}_0$. It is obvious that the grating vector $\mathbf{k}_\omega$ is equal to the grating vector $\mathbf{k}_0$. The fringe vector $\mathbf{f}_\omega$ is still orthogonal to the grating vector $\mathbf{k}_\omega$ after rotation and the following equation is satisfied.

$$\mathbf{f}_\varpi \mathbf{k}_\varpi = \mathbf{f}_{\varpi x}\mathbf{k}_{\varpi x} + \mathbf{f}_{\varpi y}\mathbf{k}_{\varpi y} + \mathbf{f}_{\varpi z}\mathbf{k}_{\varpi z} = 0 \qquad (4)$$

The common size of fringe vectors $\mathbf{f}_\omega$ is expressed as follows.

$$|\mathbf{f}_\varpi|^2 = f_{\varpi x}^2 + f_{\varpi y}^2 + f_{\varpi z}^2 = |\mathbf{f}\mathbf{f}_0|^2 \qquad (5)$$

The components of the fringe vector $\mathbf{f}_\omega$ can be decided from equations (3)-(5). Finally we can get values of the illumination vector $\mathbf{u}_\omega$ and the reconstruction vector $\mathbf{v}_\omega$ from the grating vector $\mathbf{k}_\omega$ and the fringe vector $\mathbf{f}_\omega$ as follows.

$$\mathbf{u}_\varpi = \frac{(\mathbf{f}_\varpi - \mathbf{k}_\varpi)}{2}, \mathbf{v}_\varpi = \frac{(\mathbf{f}_\varpi + \mathbf{k}_\varpi)}{2} \qquad (6)$$

The pair of $\mathbf{u}_\omega$ and $\mathbf{v}_\omega$ satisfies the same Bragg condition equ. (1) that the pair of $\mathbf{u}_0$ and $\mathbf{v}_0$ does.

In the above calculation process it is not necessary that the layers of fringes are parallel to the yz-plane. Thus this procedure of rotation is fit for arbitrary inclined fringes. Moreover we can freely select two unknowns from five factors: $\mathbf{u}$, $\mathbf{v}$, $\mathbf{u}_\omega$, $\mathbf{v}_\omega$ and ω. We can also handle each $\mathbf{u}$ or $\mathbf{v}$ for reference beam or object beam in the recording time. This theory of three-dimensional volume hologram can be applied for both reflection hologram and transmission hologram.

4. Design of Multi-View Screen

4.1 Application for hologram screen

All contents in the previous chapter are stated about the internal phenomena of volume hologram. We have to make a few more considerations in order to apply the theory of three-dimensional Bragg diffraction for multi-view hologram screen.

The first is refraction of the incident beam at the boundaries of hologram screen. The difficulty caused by refraction is shown in Fig. 3. Fig. 3 is illustrated in the expanded size for understanding the internal state of hologram screen. In Fig. 3 x-axis is vertical and parallel to the surfaces of hologram screen; y-axis is horizontal and parallel to the surfaces of hologram screen; z-axis is perpendicular to the surfaces of hologram screen. It is usual that the direction of interference fringes is different from that of the surfaces of hologram screen except for y-axis. Therefore the direction of the grating vector is not parallel to x-axis or z-axis. Moreover no vector of light rotated in the three-dimensional space is parallel to each

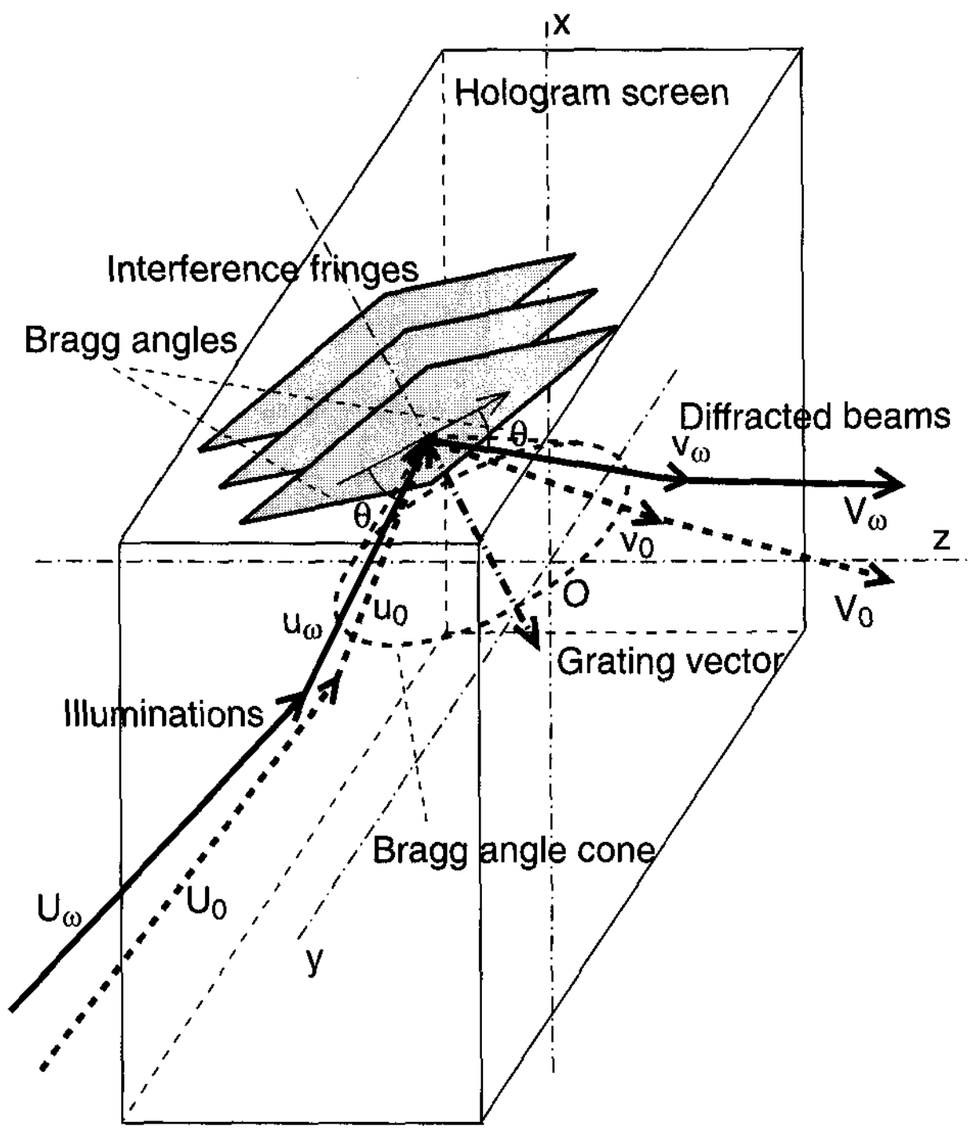

Fig. 3. Structure of hologram screen.

axis. It is then difficult to find the external direction of illumination or diffracted beam.

The usage of direction cosine is easy method to examine the refraction in the three-dimensional space. It is the reason that Snell's law can only be formulated in two-dimensional plane orthogonal to the refractive surface. Direction cosine is useful to select the section containing the optical axes of both incident light and refracted light. Fig. 4 shows Snell's law by the notation of direction cosines. The vector **e** expresses the light incident to the boundary of hologram. The vector **e** is a unit vector which direction cosines are noted by (e_x, e_y, e_z). The vector **E** expresses the light refracted from the boundary of hologram. The vector **E** is also a unit vector which direction cosines are noted by (E_x, E_y, E_z). The either of **e** or **E** belongs to the internal lights of hologram and the other belongs to the external ones. Here it is assumed that **e** is external and **E** is internal. Then Snell's law is expressed by the following equation.

$$\sqrt{e_x^2 + e_y^2} = n\sqrt{E_x^2 + E_y^2} \qquad (7)$$

where n is the refractive index of hologram. The incline of the section for Snell's law is expressed by

$$\frac{e_y}{e_x} = \frac{E_y}{E_x} \qquad (8)$$

It is obvious that the following equation is satisfied about unit vectors.

$$e_x^2 + e_y^2 + e_z^2 = E_x^2 + E_y^2 + E_z^2 = 1 \qquad (9)$$

The following relations are concluded by equations (7)-(9).

$$e_x = nE_x, e_y = nE_y$$
$$e_z = \sqrt{1-(nE_x)^2-(nE_y)^2} = \sqrt{1-n^2+(nE_z)^2} \qquad (10)$$

Equ. (10) shows Snell's law about unit vectors and it is easy to get the real vectors by multiplying size factor $2\pi n/\lambda$ or $2\pi/\lambda$ according to the internal or the external.

The other problems are the focal length of hologram screen, coloring of hologram screen, the thickness of volume hologram, the distortion of 3D image, etc. The

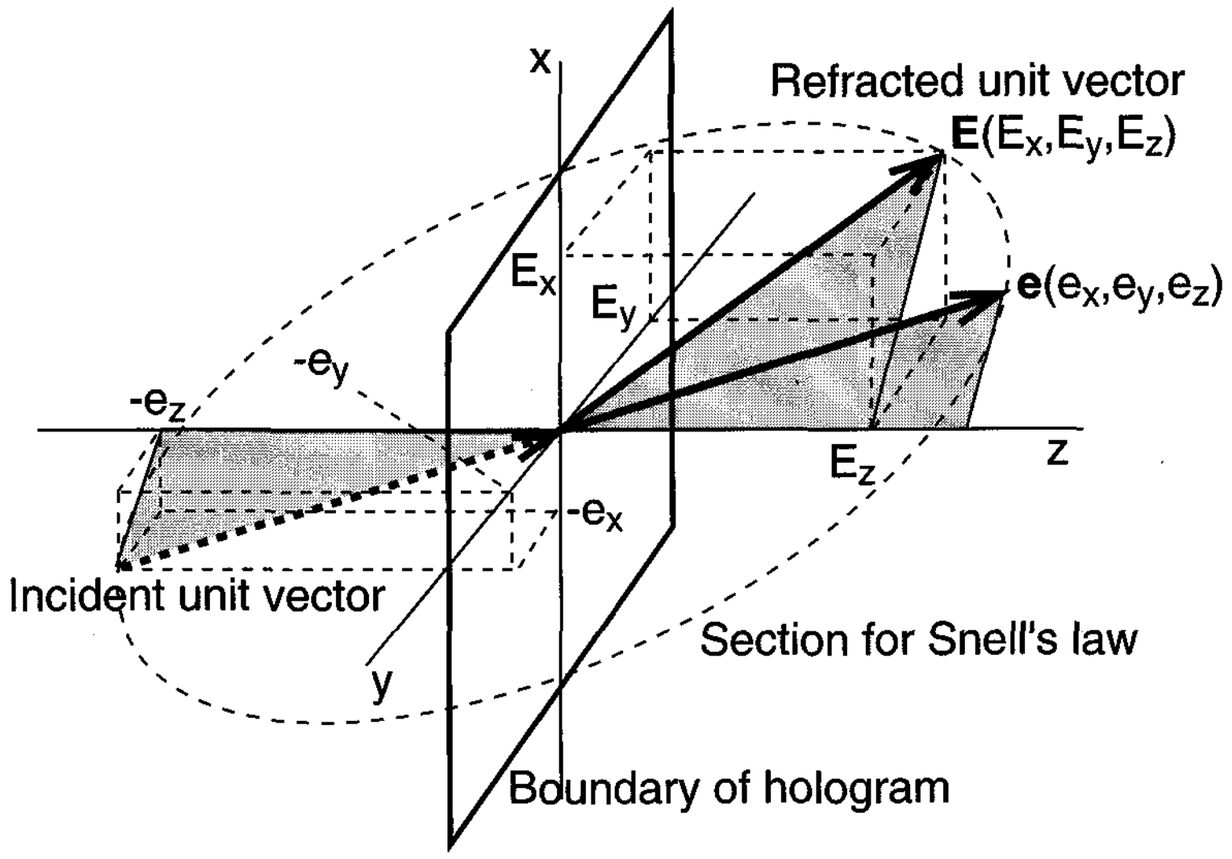

Fig. 4. Snell's law by direction cosines.

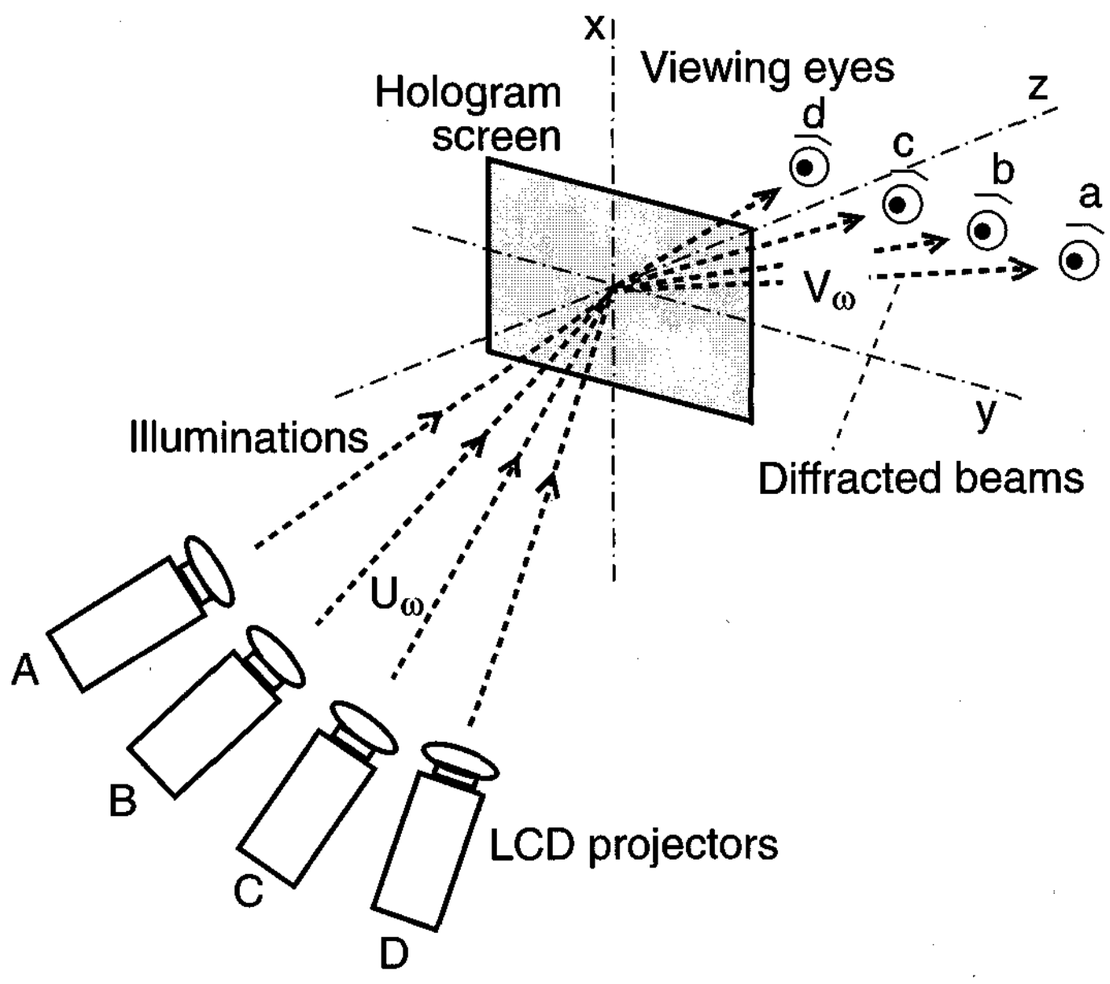

Fig. 5. Basic configuration of multi-view display.

focal length of hologram screen can be calculated by the following equation as Champagne explained [23].

$$\frac{1}{\lambda_\omega}\left(\frac{1}{V_{d\omega}}-\frac{1}{U_{d\omega}}\right)=\frac{1}{\lambda_0}\left(\frac{1}{V_{d0}}-\frac{1}{U_{d0}}\right) \tag{11}$$

where λ_0 is the wavelength, V_{d0} is the distance of object beam and U_{d0} is the distance of reference beam in the recording time; λ_ω is the wavelength, $V_{d\omega}$ is the distance of diffracted beam and $U_{d\omega}$ is the distance of illumination after rotation in the reconstruction time.

Our method to control the reconstruction color of hologram is useful for making color hologram screen by a single laser [22,24]. The essential point is to change θ instead of λ in order to record the same Λ in the Bragg condition equ. (1). The standard of incident angle to volume hologram was also shown by our previous research that the under limit of volume hologram became

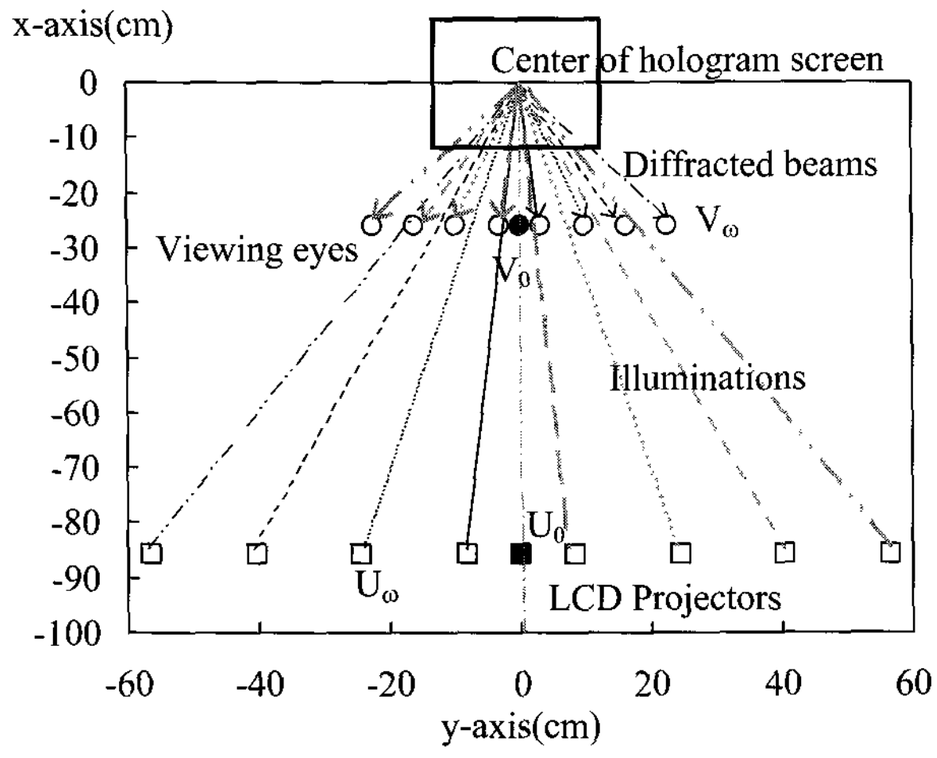

(a)

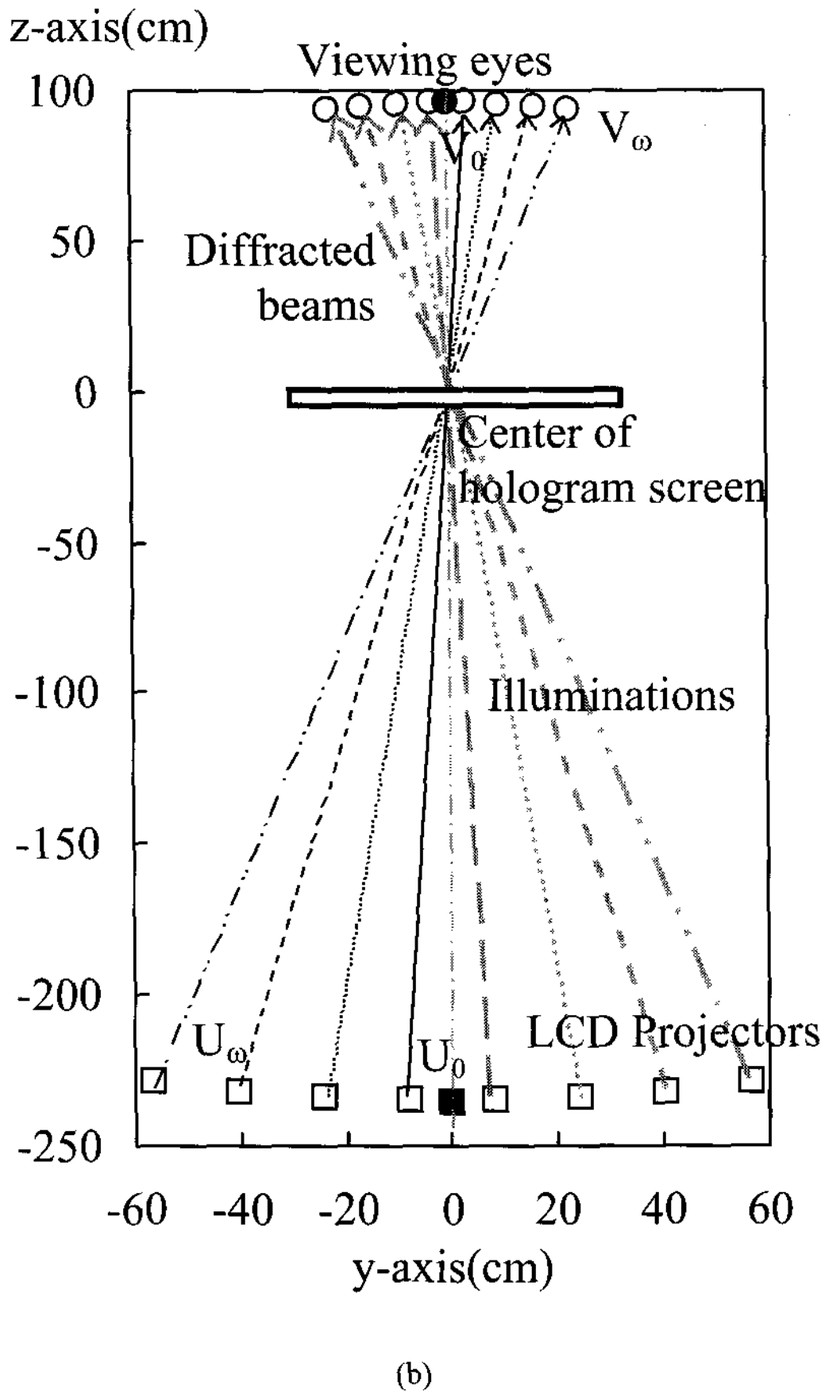

(b)

Fig. 6. Positions of viewing eyes and illuminations about multi-view display. (a) x and y coordinates of multi-view display. (b) y and z coordinates of multi-view display.

about 35 degrees [22]. This limit is about transmission hologram and there is no limit in the case of normal reflection hologram.

It is important to make the angle of illumination as small as possible for decreasing the vertical distortion of 3D image projected on hologram screen. Then it is clever to divide the under limit angle between illumination and diffracted beam in volume hologram. There is one more merit that the both angles of elevation (or inclination) about illumination and diffracted beam become the same

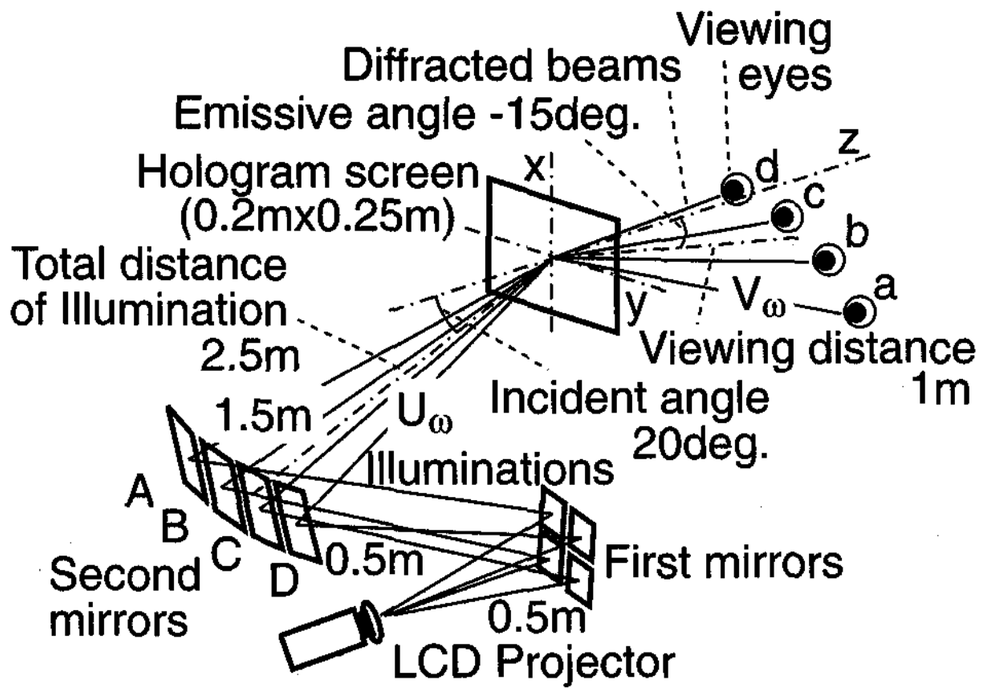

Fig. 7. Experimental display with 4 viewing points.

value and the distortion of pictures projected on the screen is counterbalanced. However it is not recommended to set the angles of illumination and diffracted beam to the perfectly same value because very complicated interference happens in the hologram material by their internal reflections. In such a case the diffraction efficiency of hologram screen is considerably degraded.

4.2 Principle of multi-view display

Fig. 5 shows a basic configuration of multi-view display with hologram screen. An example composed of 4 viewing points is illustrated. The configuration is very simple. Each liquid crystal display (LCD) projector provides two-dimensional picture which disparity slightly differs from that of the others. Each two-dimensional picture is overlaid on the hologram screen but distributed toward the viewing eye corresponding to the picture by the diffraction of hologram screen. Each viewing eye can look at only one picture; eye a looks the picture of projector A, etc. Thus the observer can look at multi-view image when he moves his eyes sideways. Here U_ω expresses the direction of illuminations and V_ω expresses the direction of diffracted beams. Three axes (x, y, z) cross at the center of hologram screen.

Next we calculate the positions of projectors and viewing eyes in order to realize the display illustrated in Fig. 5. In this case the type of hologram is transmission hologram. We set each focal length of projectors to $U_{d\omega}$= –2.5 m (negative for incident light) and each focal length of viewing eyes to $V_{d\omega}$=1 m. The angle of illumination before rotation is 20 degrees and the angle of diffracted beam before rotation is –15 degrees. As the difference between two angles becomes 35 degrees, the hologram screen belongs to volume hologram. The vertical distortion of 3D image becomes 1/cos(20 deg)=1.06 and little conspicuous.

Fig. 6 shows the result of calculation about three-dimensional Bragg diffraction. Fig. 6 (a) shows x and y coordinates. Fig. 6 (b) shows y and z coordinates. The central black mark V_0 indicates the object beam in recording time. The central black mark U_0 indicates the reference beam in recording time. Eight white marks V_ω indicate viewing eyes and eight white marks U_ω indicate illuminations. Fig. 6 (a) explains that the vertical displacement among viewing eyes is negligible and the height of viewing eyes is about –0.26 m. The vertical displacement among illuminations is also negligible and the height of illuminations is about –0.86 m. Fig. 6 (b) shows interesting result that the curve of viewing eyes forms a circumference. Its center exists on the x-axis through the center of hologram screen and its horizontal radius is about 0.97 m. Fig. 6 (b) also illustrates a similar circumference of illuminations which horizontal radius is about –2.35 m. These results indicate that the combination of illuminations and viewing eyes forms the Bragg angle cone. Moreover each curve of illuminations or viewing eyes becomes latitude of the Bragg angle cone.

By the way, the interval of viewing eyes V_ω in Fig. 6 (b) is 0.065 m that is the average inter-pupil distance of adult. The interval of illuminations U_ω in Fig. 6 (b) is

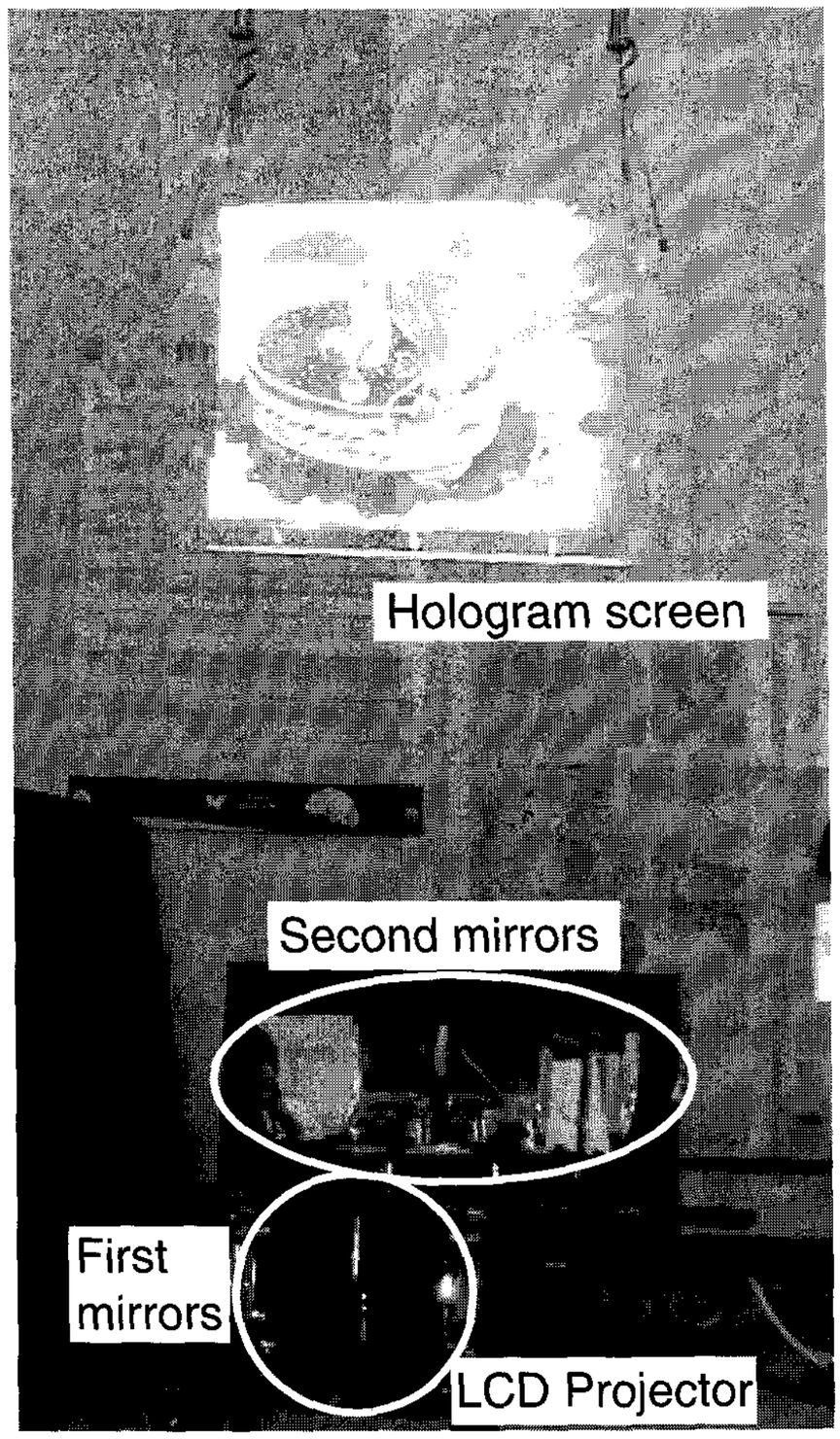

Fig. 8. Picture of experimental display with 4 viewing points.

corresponding to that of V_ω. Then the observer can look multi-view image when illuminations are located on the marks of U_ω.

5. Experiments

We developed a trial device with 4 viewing points as is illustrated in Fig. 7. The fundamental specifications are the same values as we explained in the previous chapter. Instead of 4 projectors we used a projector and arrays of optical mirrors. The hologram screen is made of a PFG-03C plate and its size is 0.2 m by 0.25 m. The refractive index of hologram plate is assumed n=1.63 [25]. The recording wavelength is 532 nm (green) and the designed wavelengths about the diffracted beams are 620 nm (red), 532 nm (green) and 465 nm (blue) for good color reappearance [22,26].

If the focus of diffracted beam is a small point actually, the observer feels difficulty to adjust his eyes to such focuses. Then the real object beam is made of a diffusion plate which size is 0.15 m by 0.04 m. The diffusion plate is effective to cover the difference of each individual inter-pupil distance.

Fig. 8 shows a picture of the trial device. Extremely bright 3D image is reconstructed on the hologram screen. Optical devices are located at the bottom. The first mirrors are dark because only the backs can be seen. A part of the light from LCD projector is found behind the first mirrors.

Fig. 9 shows 4 pictures of 3D image displayed on the hologram screen every 4 viewing points. All of them are very clear and bright because any direction satisfies the Bragg condition. The vertical distortion of 3D image is also sufficiently small though the pictures are skewed because of camera angle.

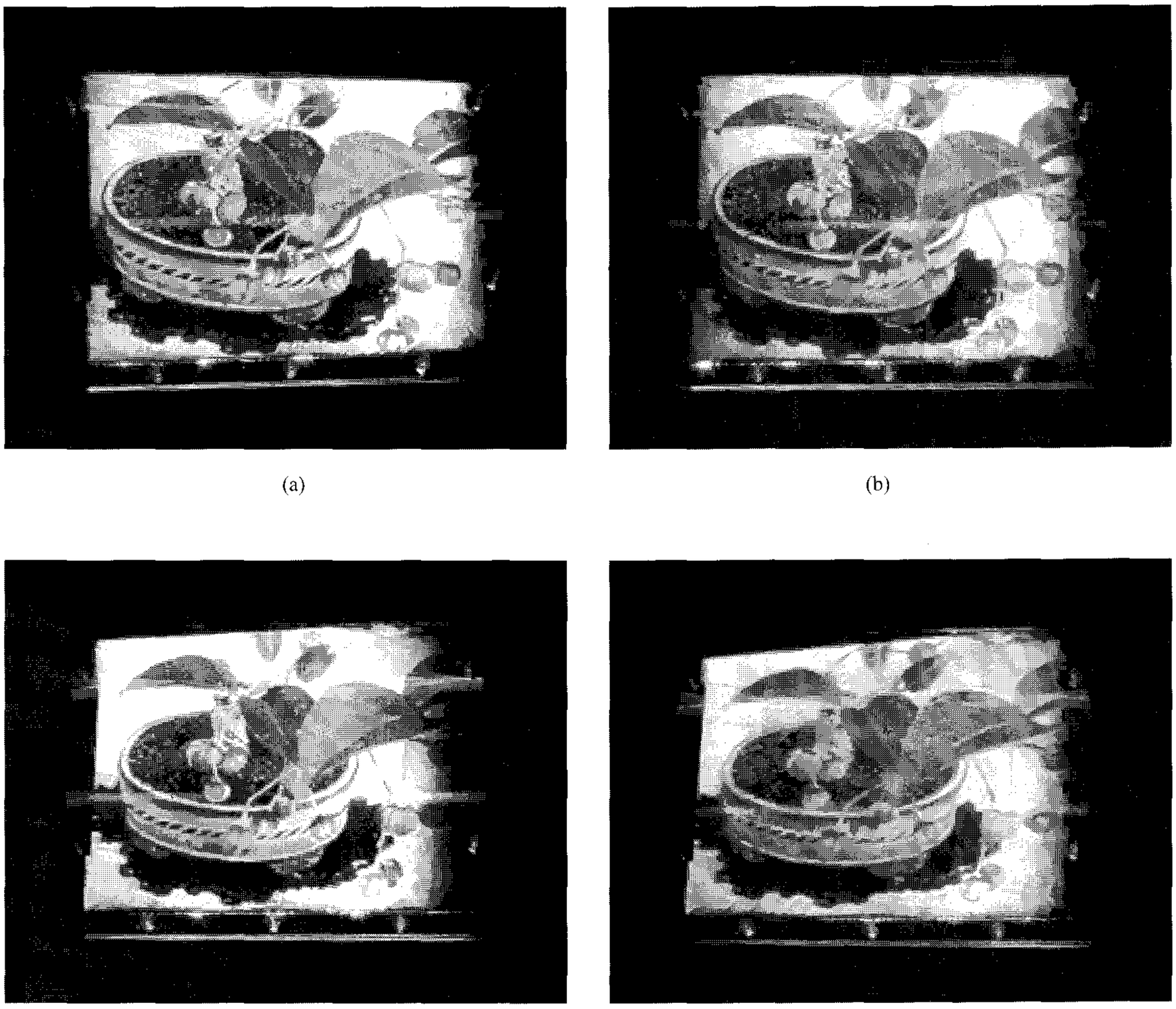

(a) (b)

(c) (d)

Fig. 9. Pictures of multi-view image displayed on the hologram screen. (a) End of the left. (b) Middle of the left. (c) Middle of the right. (d) End of the right.

6. Conclusions

We introduced the method to extend the theory of the Bragg diffraction to the three-dimensional space. We explained the algorithm to convert the directions of a pair of illumination and diffracted beam under the condition that the direction of the grating vector was preserved. Moreover we indicated a design of multi-view display with hologram screen that could be multiple reconstructed in spite of single recording. This hologram screen is able to answer arbitrary numbers of viewing points within wide viewing zone. We actually achieved an experimental device of 4 viewing points. We could also make the vertical distortion of 3D image sufficiently small by dividing the cross angle between illumination and diffraction beam.

References

[1] J. S. Kollin, S. A. Benton, and M. L. Jepsen, Proc. SPIE, **1136**, 178 (1989).

[2] N. Hashimoto, K. Hoshino, and S. Morokawa, Proc. SPIE, **1667**, 2 (1992).

[3] K. Taima, H. Ueda, H. Okamoto, T. kubota, Y. kajiki, T. Nakamura, H. Nishida, H. Takahashi, and E. Shimizu, Proc. SPIE, **2176**, 23 (1994).

[4] J. H. Kulick, S. T. Kowel, G. P. Nordin, A. Parker, R. Lindquist, P. Nasiatka, and M. Jones, Proc. SPIE, **2176**, 2 (1994).

[5] M. Shires, Proc. SPIE, **2333**, 381 (1994).

[6] T. Toda, S. Takahashi, and F. Iwata, Proc. SPIE, **2406**,

191 (1995).
[7] D. Trayner and E. Orr, Proc. SPIE, **2653**, 65 (1996).
[8] K. Sakamoto, H. Takahashi, E. Shimizu, H. Ueda, K. Tanaka, and M. Okamoto, Proc. SPIE, **3011**, 36 (1997).
[9] C. Newswanger, U. S. Patent 4799739, (Jan. 24, 1989).
[10] P. Hariharan, Optical Holography, Cambridge University Press (Second Edition, 1996).
[11] M. Okamoto, K. Yamasaki, and E. Shimizu, Proc. SPIE, **3293**, 48 (1998).
[12] M. Okamoto, T. Ando, K. Yamasaki, and E. Shimizu, Proc. 3D Image Conference '99, 99 (1999) [in Japanese].
[13] M. Okamoto and E. Shimizu, J. of the Institute of Image Electronics Engineers of Japan, **31(1)**, 43 (2002). [in Japanese].
[14] M. Okamoto, Z. Wei, and E. Shimizu, Proc. 3D Image Conference 2001, 125 (2001). [in Japanese].
[15] M. Okamoto and E. Shimizu, HODIC Circular, **21(4)**, 7 (2001). [in Japanese].
[16] W. L. Bragg, Nature, **143**, 678 (1939).
[17] W. L. Bragg, Nature, **149**, 470 (1942).
[18] H. Kogelnik, The Bell System Technical J., **48(9)**, 2909 (1969).
[19] E. G. Ramberg, RCA Rev., **27**, 467 (1966).
[20] G. Saxby, Practical Holography, Prentice Hall, (Second Edition, 1994).
[21] S. A. Benton, International Symposium on Display Holography, **3**, 593 (1988).
[22] M. Okamoto, T. Ando, K. Yamasaki, and E. Shimizu, Proc. SPIE, **3956**, 64 (2000).
[23] E. B. Champagne, J. Opt. Soc. Am., **57(1)**, 51 (1967).
[24] M. Okamoto and E.Shimizu, Proc. 2nd IMID, 1005 (2002).
[25] H. I. Bjelkhagen, Silver-Halide Recording Materials for Holography and Their Processing, Springer-Verlag, (1993).
[26] K. Ohnuma and F. Iwata, Appl. Opt., **27(18)**, 3859 (1988).